Rock and Soil Mechanics

Volume 41 | Issue 3 Article 6

9-27-2020

Experimental investigation on the dynamic response of pile group foundation on liquefiable ground subjected to horizontal and vertical earthquake excitations

Heng-yuan ZHANG

De-ling QIAN
dlqian@sina.com

Chao SHEN

Qi-quan DAI

Custom Citation

ZHANG Heng-yuan, QIAN De-ling, SHEN Chao, DAI Qi-quan. Experimental investigation on the dynamic response of pile group foundation on liquefiable ground subjected to horizontal and vertical earthquake excitations[J]. Rock and Soil Mechanics, 2020, 41(3): 905-914.

Rock and Soil Mechanics 2020 41(3): 905−914 ISSN 1000−7598
https: //doi.org/10.16285/j.rsm.2019.5306 rocksoilmech.researchcommons.org/journal

Experimental investigation on the dynamic response of pile group foundation on liquefiable ground subjected to horizontal and vertical earthquake excitations

ZHANG Heng-yuan, QIAN De-ling, SHEN Chao, DAI Qi-quan
College of Civil Engineering, Hefei University of Technology, Hefei, Anhui 230009, China

Abstract: To investigate the dynamic response of pile group foundation on liquefiable ground subjected to horizontal and vertical (bidirectional) coupling earthquake excitations, a shaking table model test for a dynamic interaction system with liquefiable ground −pile group foundation−frame tube structure was conducted. Different types of earthquake motions were selected as the excitations for the shaking table test, and then the influence of bidirectional coupling earthquake excitations on the dynamic response of liquefiable ground and pile group foundation were analyzed by comparing the test results of soil acceleration, excess pore water pressure and pile group strain subjected to horizontal unidirectional and bidirectional coupling excitations. The results indicate that under the bidirectional coupling earthquake excitations, the vertical peak acceleration of liquefiable soil gradually increases with the decrease of buried depth; the liquefaction effect of saturated sand is related to the bidirectional coupling earthquake excitations and the type of input earthquake motions; besides, compared with the horizontal earthquake excitation, the peak strain in the central and bottom of pile group foundation are larger those under the bidirectional coupling earthquake excitations, the variation of peak strain of pile top is different; also, the swaying and tilting of the pile group system of the building structure are exacerbated by the bidirectional coupling earthquake excitations. The research results are of great significance to both the seismic design of pile group on liquefiable foundation and disaster prevention and mitigation.

Keywords: horizontal and vertical earthquake excitations; shaking table test; liquefaction; pile-soil-structure dynamic interaction; dynamic response

1 Introduction

Earthquakes are one of the major natural disasters suffered by human beings. In recent years, there have been frequent earthquakes and active crustal movements worldwide, resulting in a series of serious casualties and economic losses. The traditional view is that horizontal earthquake excitations is the decisive factor that causes damage to geotechnical structures. However, recent earthquake damage survey results indicate that[1−2], for some earthquakes in high intensity area, the vertical acceleration even exceeds the horizontal acceleration. The combined effect of horizontal and vertical earthquake excitations exacerbates the destruction of geotechnical structure. Farsangi[3], Chen[4], Tan[5], Zhang[6] and other scholars have studied the dynamic response and seismic performance of frame, bridge, high-rise, isolated structure and other structural systems under combined effect of horizontal and vertical earthquake excitations. Existing literature shows that the research on the dynamic response of superstructure under the horizontal and vertical earthquake excitations is deep and fruitful.

Most of the above studies were carried out based on the assumption of rigid foundations. In fact, the ground-foundation-superstructure vibrates as a whole, which will cause mutual influence and restraint[7]. Underground pile foundation mainly bears the self-weight of the superstructure. Under the combined effects of the horizontal and vertical earthquake excitations, the behavior of pile foundation becomes very complicated under the consideration of the foundation liquefaction. In many cases, damage and collapse of buildings are also caused by the failure of ground and foundation. Therefore, the study on dynamic response of liquefiable ground and underground foundation under combined effect of horizontal and vertical earthquake excitations cannot be ignored. Based on the OpenSees finite element earthquake simulation platform, Wang et al.[8] studied the combined effects of the horizontal and vertical earthquake excitations on the dynamic response of the liquefiable ground-pile-bridge structure system using OpenSees. Tsaparli et al.[9] studied the effect of vertical acceleration on site liquefaction through the ICFEP finite element program. Guo et al. (2002) considered the effect of horizontal and vertical coupling earthquake excitations on the failure of underground structure, and analyzed the failure of underground structure through the finite difference program FLAC. The above related researches and conclusions are mostly limited to the numerical simulation method, and the

Received: 30 January 2019 Revised: 5 June 2019
This work was supported by the National Nature Science Foundation of China(51378168).
First author: ZHANG Heng-yuan, male, born in 1993, Master degree candidate, majoring in structural seismic and soil-structure dynamic interaction. E-mail: hyzhanghfut@foxmail.com
Corresponding author: QIAN De-ling, female, born in 1956, PhD, Professor, doctoral supervisor, research interests: geotechnical engineering. E-mail: dlqian@sina.com

experimental research on the dynamic response of pile group foundation of building structures on the liquefiable foundation under horizontal and vertical coupling earthquake excitations is still rare. With the rapid development of cities and the restriction of land resources, the frame-core tube structures are widely used. It is of great significance to study the dynamic response of pile group foundation of frame-core tube structure in liquefiable ground subjected to horizontal and vertical earthquake excitations.

In view of this, shaking table test is used to simulate the dynamic response of liquefiable soil-pile group-frame tube structure under earthquake excitations. Shaking table test results under horizontal earthquake excitations alone (hereinafter referred to as "horizontal earthquake excitations") and horizontal and vertical coupling earthquake excitations (hereinafter referred to as "bidirectional coupling earthquake excitations"), are compared to study the influence of bidirectional coupling earthquake excitations on the dynamic response of liquefiable foundation and pile group foundation.

2 Shake table test

2.1 Similitude law for model design

The shaking table test model was designed using similitude law, and the test was conducted at the State Key Laboratory of Disaster Reduction in Civil Engineering of Tongji University. Based on comprehensive consideration of the shaking table performance parameters, the boundary effect of soil box, test site conditions and other factors, and combined with Buckingham π theorem, the dynamic similitude ratio of the test model structure was determined. For the major controlling parameters, the length similarity ratio S_L = 1/50, the elastic modulus similarity ratio S_E = 1/3 and the acceleration similarity ratio S_a = 3.8, and the dynamic similitude relationship and similitude ratio of other major physical quantities are shown in Table 1.

Table 1 Similitude relationships for model shaking table test

Similitude relationship	Formula	Similitude ratio
Length S_L	S_L	1/50
Poisson's ratio S_μ	S_μ	1
Elastic modulus S_E	S_E	1/3
Stress S_σ	$S_\sigma = S_E$	1/3
Strain S_ε	$S_\varepsilon = S_\sigma / S_E$	1
Acceleration S_a	S_a	3.8
Mass density S_ρ	$S_\rho = S_E/(S_a S_L)$	4.39
Mass S_m	$S_m = S_\sigma S_L^2 / S_a$	1/28 500
Stiffness S_k	$S_k = S_E S_L$	1/150
Time S_t	$S_t = (S_L/S_a)^{0.5}$	0.072 5
Velocity S_V	$S_V = (S_L S_a)^{0.5}$	0.276
Frequency S_ω	$S_\omega = (S_a/S_L)^{0.5}$	13.78

2.2 Soil properties and boundary conditions

The test site soils were divided into 3 layers, including silty clay layer, sand layer and gravel layer from top to bottom. The silty clay had a thickness of 0.1 m, a dry density of 1.54 g /cm^3, a plastic limit of 17.1% and a liquid limit of 27.4%. The thickness of sand layer was 0.5 m, and the sand used was a fine sand, and the grain size distribution of fine sand is shown in Fig.1. The thickness of the gravel layer was 0.5 m and the maximum grain size is 10 mm. The foundation soil for the test model was filled uniformly by layers. The relative density D_r of the sand layer was controlled to be 45% – 50% during the filling process, and the water level line was located at the boundary between the silty clay layer and the sand layer.

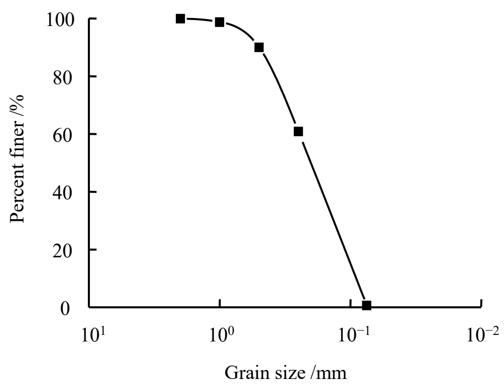

Fig.1 Grain size distribution of fine sand

As we all know, the foundation soil of building is infinite in reality. However, for large-scale shaking table test, considering the bearing capacity of shaking table and the limit of test space, it is difficult to simulate the infinite foundation soil in shaking table test. Therefore, flexible or laminar soil box with a size much larger than the structural model is typically used as the artificial boundary in the soil–structure dynamic interaction shaking table test. In order to reduce the "model box effect", a flexible cylinder container with a diameter of 3.0 m and a height of 1.5 m was used as the boundary condition of the test soil in this experiment, and its effectiveness has been proved from the literature [11].

2.3 Model design and construction

The upper structure and lower pile group foundation of the test model were made of concrete and galvanized iron wire. According to the dynamic similitude ratio determined by the test model and combined with the layer extraction method, the height of the upper frame-core tube after fabrication was 3.566 m, and the total additional weight of the floor was 17.8 kN.

According to the dynamic similitude relationship, the equivalent stiffness principle and "*Technical code for building pile foundations* " (JGJ94 2008)[12], the pile foundation of the prototype building was simplified as a 3×3 pile group foundation. The model pile had a diameter of 8 cm, pile length of 72 cm, main reinforcement 8ϕ4, stirrup ϕ0.9@10, pile spacing of 34 cm, platform size of 92 cm × 92 cm, and the bottom of the pile was embedded in the bottom gravel layer, and the embedded length was 2.75 times the pile diameter. The details of the shaking table test model design were reported in the literatures[13–14]. The arrangement of pile group is shown in Fig.2, and the shaking table test model after fabrication is shown in Fig.3.

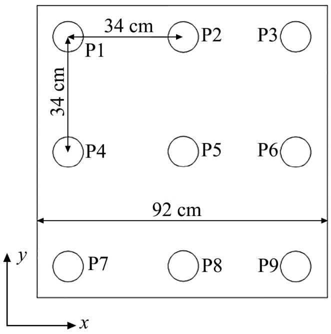

Fig.2 Arrangement of pile group

Fig.3 Shaking table test model

2.4 Instrumentation layout

In the shaking table test, the acceleration sensors were used to measure the acceleration response of liquefiable ground and pile group foundation. The strain gauges were attached evenly along the height of pile to measure the strain change of pile, the earth pressure boxes were buried at the soil-pile interface to measure the contact pressure, and the pore water pressure gauges were buried at different locations of the liquefiable foundation to measure the change of pore water pressure in the foundation soil. The strain gauges were resistance type strain gauge, the earth pressure boxes were resistance type sensor with measuring range up to 0.5 MPa, the pore water pressure sensors were resistance type dynamic osmometer with measuring range up to 50 kPa, and the layout of test sensors is shown in Fig.4.

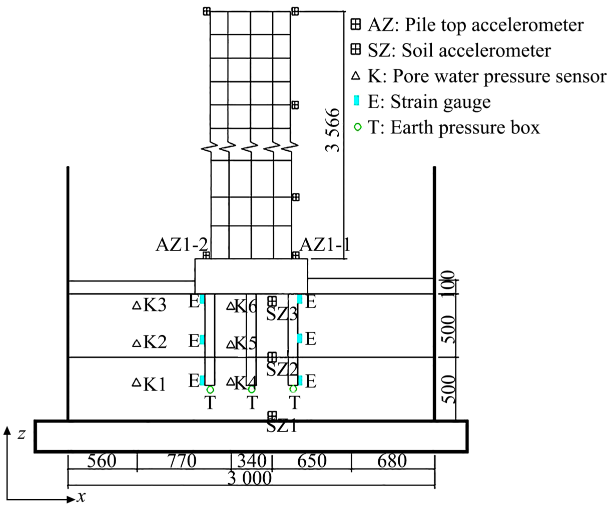

Fig.4 Layout of sensors (unit: mm)

2.5 Testing scheme

The unidirectional and bidirectional input earthquake motions for the shaking table were selected from two real earthquake motions (El-Centro motion and Kobe motion), and the peak acceleration and time interval of the earthquake motions were adjusted according to the dynamic similitude ratio determined by the test. In order to simulate VII and VIII magnitude earthquake excitations, the peak accelerations of the input earthquake motions for the shaking table were adjusted to 0.38*g* and 0.76*g*, respectively. In recent years, seismic records have shown that larger vertical acceleration peaks are often accompanied with larger horizontal accelerations. Therefore, in the bidirectional coupling earthquake excitations, the same input peak acceleration were selected for the *X* and *Z* directions.

Time–history plots of the El-Centro motion and the Kobe motion with a peak acceleration of 0.38*g* are shown in Fig.5. After the earthquake excitation application of the previous test condition, and the pore water pressure was essentially dissipated, then the earthquake excitation application of the latter test condition was carried out. The earthquake excitation application scheme is shown in Table 2.

3 Liquefiable site response

3.1 Site vertical acceleration

The test data was processed and analyzed, and the vertical acceleration time–history plots and Fourier spectra at the different depths (SZ1–SZ3) of the same horizontal location in the foundation were obtained. The test results show that the acceleration variations of vertical vibration along the buried depth of soil are similar under the bidirectional coupling earthquake excitations with different intensities and different earthquake excitations. Limited to the length of the paper, this

Rock and Soil Mechanics, Vol. 41 [2020], Iss. 3, Art. 6

section only presents the time–history plots and Fourier spectra of vertical acceleration of the soil at the measuring points of SZ1–SZ3 under El-Centro bidirectional coupling earthquake excitations at 0.76*g*, as shown in Fig.6.

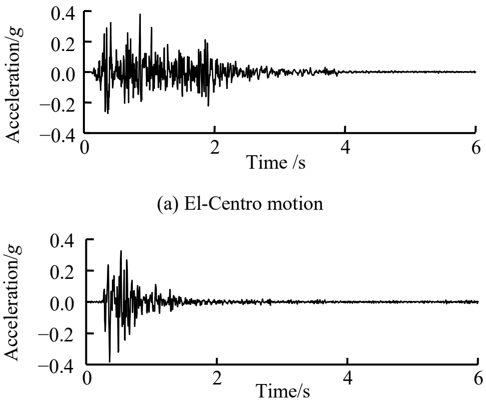

(a) El-Centro motion

(b) Kobe motion

Fig.5 Input earthquake motions for shaking table test

Table 2 Earthquake excitation application scheme

Shaking event	Input earthquake motion	Peak acceleration /*g*	
		X-direction	*Z*-direction
1	WN	0.07	—
2	El-Centro	0.38	—
3	Kobe	0.38	—
4	ElZ-Centro	0.38	0.38
5	Kobe*Z*	0.38	0.38
6	WN	0.07	—
7	El-Centro	0.76	—
8	Kobe	0.76	—
9	ElZ-Centro	0.76	0.76
10	Kobe*Z*	0.76	0.76
11	WN	0.07	—

Note: El-Centro represents El Centro motion (*X* direction); ElZ-Centro represents El Centro motion (*X, Z* direction); Kobe represents Kobe motion (*X* direction); KobeZ represents Kobe motion (*X, Z* direction); WN represents white noise.

It can be seen from Fig.6 that under the bidirectional coupling earthquake excitations of the El-Centro motion at 0.76*g*, with the increase of the distance from the measuring point to the bottom of the container, the peak vertical acceleration of the soil gradually increases, in which the peak vertical acceleration at the upper part of the foundation (at SZ3) increases the most by 60.5% (the peak vertical acceleration at the SZ3 measuring point is the peak vertical acceleration measured compared to the bottom plate of the container.). This shows that the foundation soil has an amplification effect on the transmission of vertical vibration under the bidirectional coupling earthquake excitations.

In addition, by comparing the Fourier spectra of vertical acceleration at different elevations of soil, it can be seen that although the peak value of acceleration increases significantly during the transmission of vertical vibration from bottom to top of soil, the spectrum characteristics of Fourier spectrum show no obvious change. The test soil only amplifies the vertical vibration to some extent but does not significantly change the spectrum characteristics of vertical vibration.

3.2 Excess pore water pressure

Four pore water pressure sensors with high-sensitivity were placed in the saturated sand layer to measure the change of the pore water pressure in the sand layer under the bidirectional coupling earthquake excitations. Figures 7 and 8 show the time-history plots of excess pore water pressure at each measurement point of the sand layer under the El-Centro and Kobe earthquake excitations at peak acceleration of 0.76*g*, respectively.

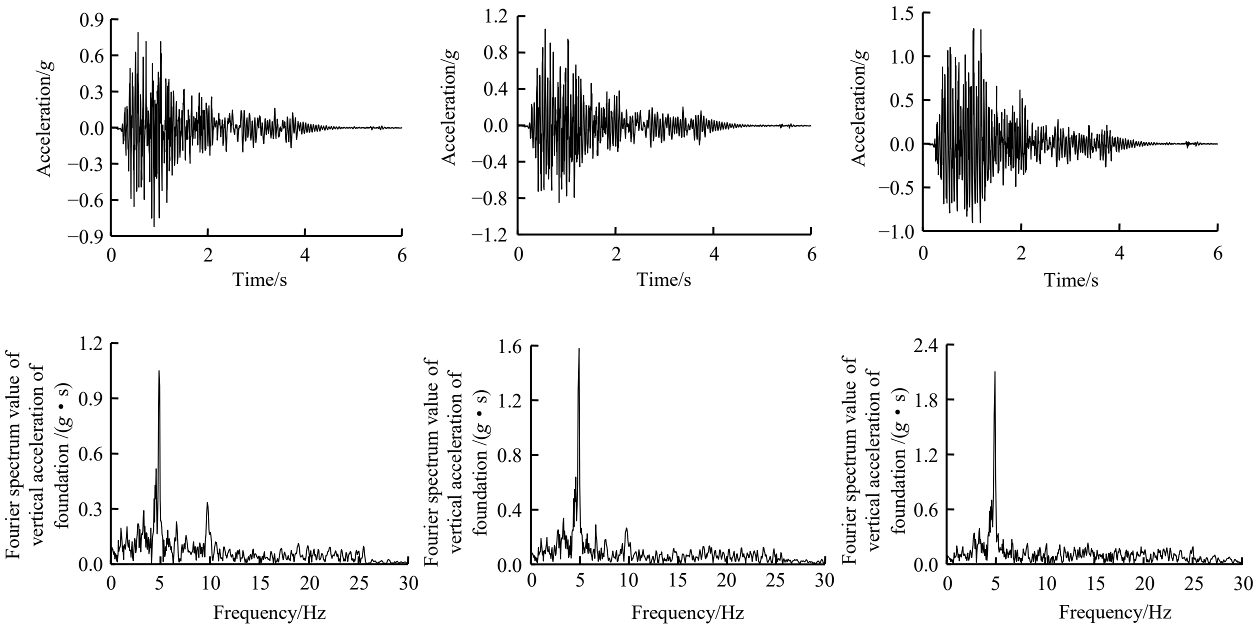

(a) SZ1 (b) SZ2 (c) SZ3

Fig.6 Acceleration response and Fourier spectra of foundation under El-Centro bidirectional coupling excitations at 0.76*g*

https://rocksoilmech.researchcommons.org/journal/vol41/iss3/6
DOI: 10.16285/j.rsm.2019.5306

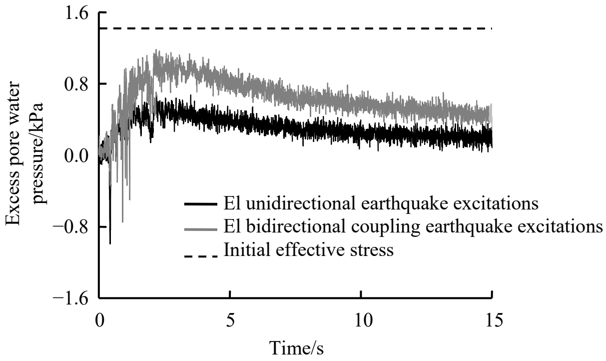

(a) K3 under El earthquake excitation

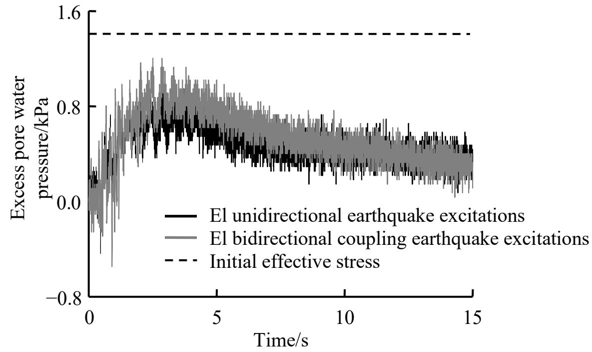

(b) K6 under El earthquake excitation

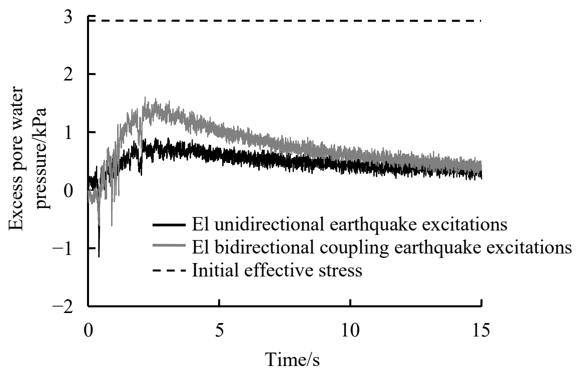

(c) K2 under El earthquake excitation

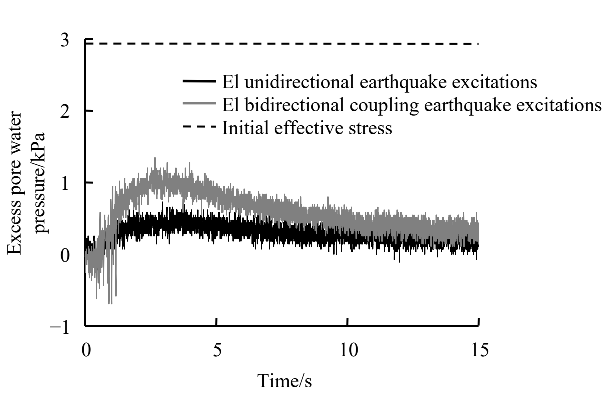

(d) K5 under El earthquake excitation

Fig.7 Time-history plots of excess pore water pressure under El-Centro earthquake excitation at 0.76*g*

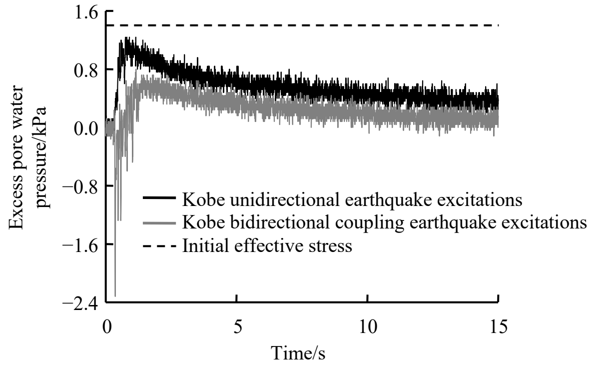

(a) K3 under Kobe earthquake excitation

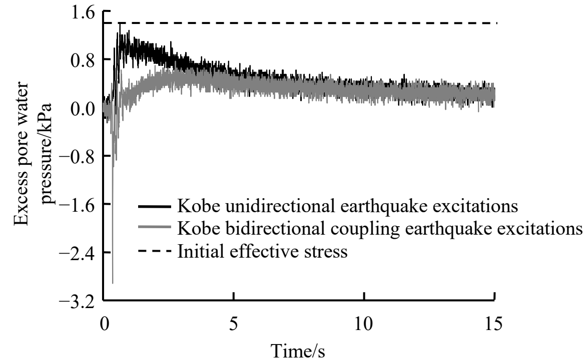

(b) K6 under Kobe earthquake excitation

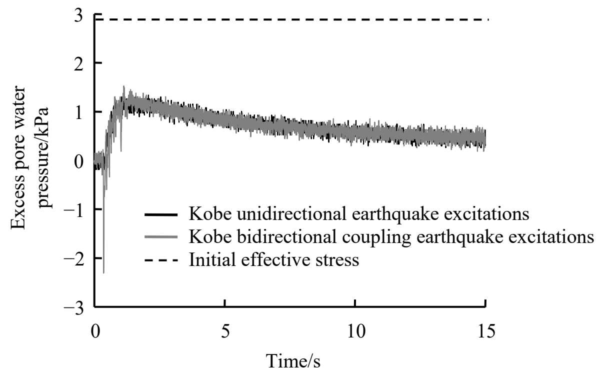

(c) K2 under Kobe earthquake excitation

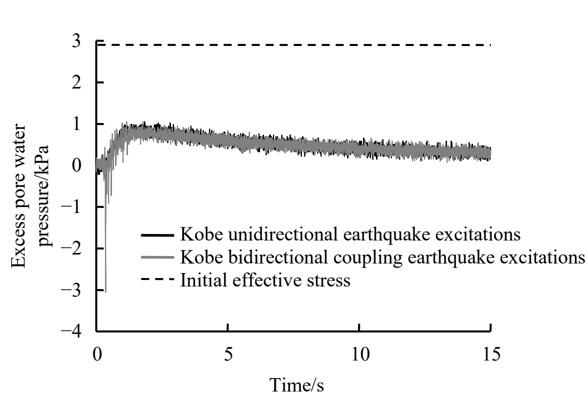

(d) K5 under Kobe earthquake excitation

Fig.8 Time-history plots of excess pore water pressure under Kobe earthquake excitation at 0.76*g*

As can be seen from Figs.7(a)–7(d), compared with El-Centro horizonal earthquake excitations at 0.76*g*, the peak value of excess pore water pressure in saturated sand layer increases significantly under El-Centro bidirectional coupling earthquake excitations at 0.76*g*. The peak values of excess pore water pressure at K3 and K6 measuring points at the depth of 0.2 m increased from 0.76 kPa and 0.94 kPa to 1.24 kPa and 1.21 kPa, respectively, with an increase of about 29%–63%; The peak values of excess pore water pressure at K2 and K5 measuring points at the buried depth of 0.5 m increased from 0.93 kPa and 0.95 kPa to 1.64 kPa and 1.35 kPa, respectively, with an increase of about 42%–76%. This indicates that the El-Centro bidirectional coupling earthquake excitations at 0.76*g* promotes the liquefaction of saturated sand layer.

From the comparison and analysis of Figs.8(a)–8(d), compared with Kobe horizonal earthquake excitations at 0.76*g*, it can be seen that the "negative pore pressure" phenomenon of saturated sand layer is obvious under the Kobe bidirectional coupling earthquake excitations at 0.76*g*, but the positive peak value of excess pore water pressure of sand layer does not increase significantly, and even decreases at the buried depth of 0.2 m. According to the relevant literature research results[15–17], the phenomenon of “instantaneous negative value” of the excess pore water pressure in saturated sand layer is caused by instantaneous shear dilation effect of saturated sand at the moment of initial peak acceleration of earthquake motions. Compared with unidirectional horizontal earthquake excitations, the instantaneous shear dilation effect of saturated sand at the initial peak acceleration moment of earthquake motions under Kobe bidirectional coupling earthquake excitations is larger, and the phenomenon of “instantaneous negative value” of pore pressure of soil is significant.

The variation of excess pore water pressure in saturated sand layer under the El-Centro and Kobe earthquake excitations at 0.36*g* is similar to that under the El-Centro and Kobe earthquake excitations at 0.76g. Therefore, in summary, under the input of El-Centro earthquake motion, the bidirectional coupling earthquake excitation has a promoting effect on sand liquefaction, while under the input of Kobe earthquake motion, the bidirectional coupling earthquake excitation has little effect on the increase of excess pore water pressure. This indicates that the liquefaction effect of soil and the increase of pore water pressure are not only affected by bidirectional coupling earthquake excitations, but also by the type of input earthquake motions.

4 Dynamic response of pile foundation

4.1 Pile strain

The strain variation amplitude of pile at each measuring point can be calculated by the test results of pile strain gauge, and the damage of pile foundation can be investigated by considering the location of the measuring point at the pile. The strain amplitude curves of P1 and P3 piles under different types of earthquake excitations are plotted as shown in Fig.9 and Fig.10.

It can be seen from Fig.9 that the strain amplitude at the middle and bottom of P1 and P3 piles increases, and the strain amplitude at the top of pile changes little under the Kobe bidirectional coupling earthquake excitations, compared with that under unidirectional horizontal earthquake excitations. The damage of the middle and the bottom of the pile is aggravated by the Kobe bidirectional coupling earthquake excitations.

It can be seen from Fig.10 that the strain amplitudes at the middle and bottom of P1 and P3 piles under El-Centro bidirectional coupling earthquake excitations are larger than those at the corresponding parts under the horizontal earthquake excitations, but the change of strain amplitudes at P1 and P3 pile top positions is quite different, specifically, the El-Centro bidirectional coupling earthquake excitations reduce the strain amplitudes at P1 pile top and increase the strain amplitudes at P3 pile top, which may be the result of the combined effect of soil liquefaction and inertial force of the superstructure.

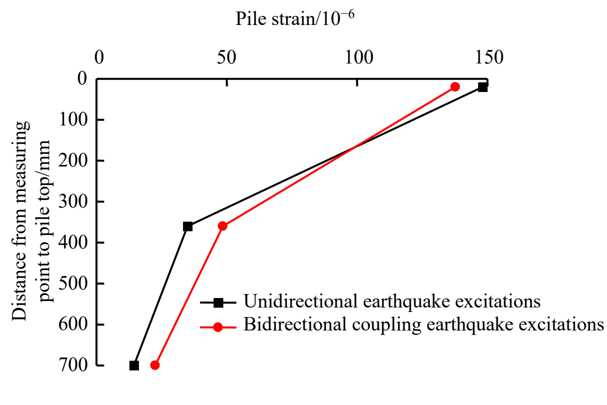

(a) P1 pile under Kobe earthquake excitation at 0.38*g*

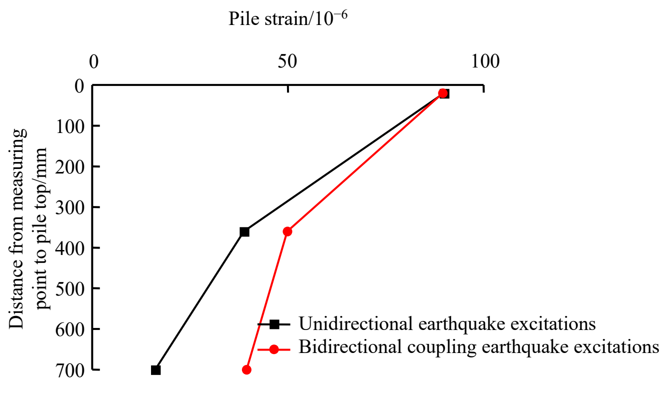

(b) P3 pile under Kobe earthquake excitation at 0.38*g*

DOI: 10.16285/j.rsm.2019.5306

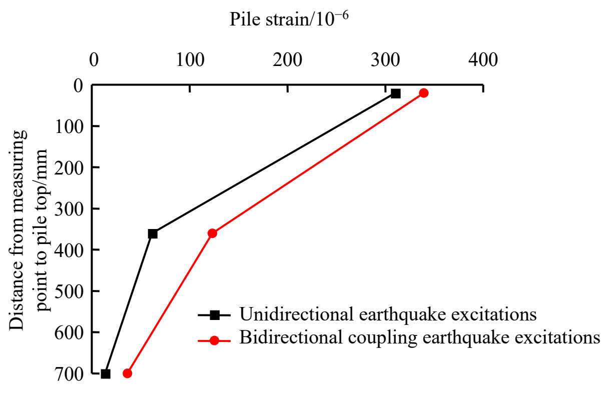

(c) P1 pile under Kobe earthquake excitation at 0.76*g*

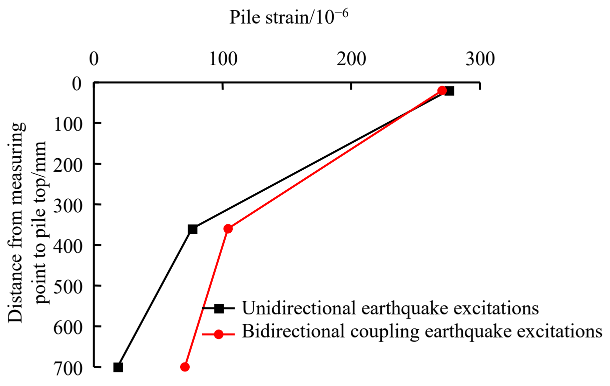

(d) P3 pile under Kobe earthquake excitation at 0.76*g*

Fig.9 Pile strain amplitude curves under Kobe earthquake excitation

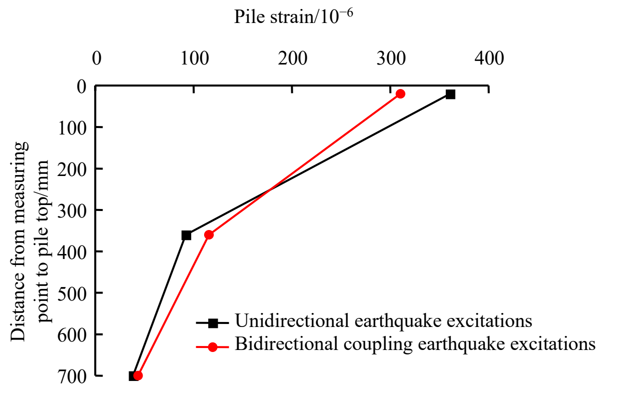

(c) P1 pile under El-Centro earthquake excitation at 0.76*g*

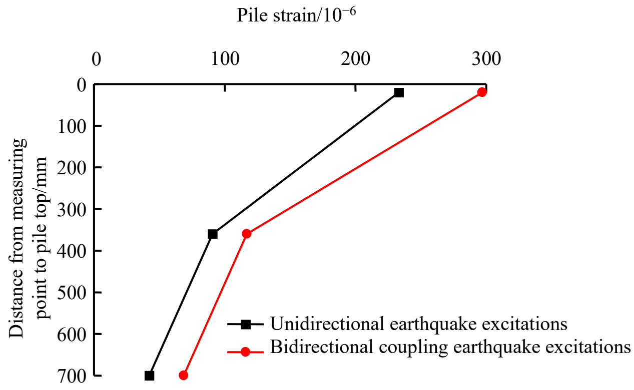

(d) P3 pile under El-Centro earthquake excitation at 0.76*g*

Fig.10 Pile strain amplitude curves under El-Centro earthquake excitation

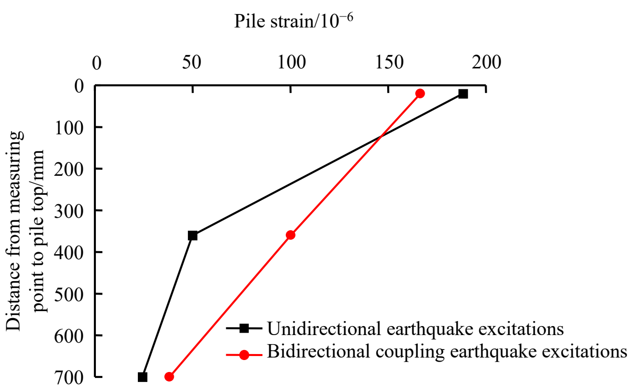

(a) P1 pile under El-Centro earthquake excitation at 0.38*g*

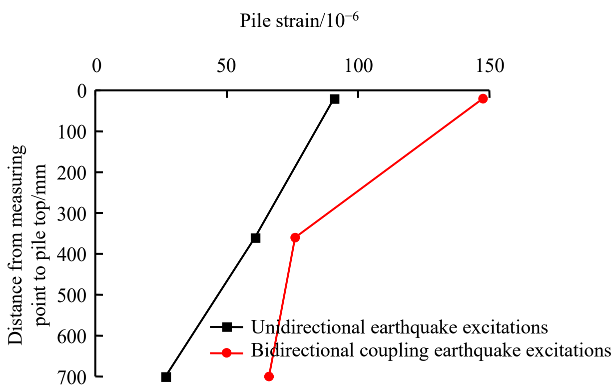

(b) P3 pile under El-Centro earthquake excitation at 0.38*g*

4.2 Earth pressure under corner pile

During the earthquake excitations, the change of the earth pressure at the bottom of the corner pile can directly reflect the uplift and tension compression effects of the pile group. Figure11 shows the time history plots of the earth pressure at the bottom of the corner piles of P1, P3 and P7, P9 on both sides of the pile group foundation under the El-Centro earthquake excitations with the peak acceleration of 0.76*g*.

According to the analysis of Figs.11(a) and (c), the time history plots of the earth pressure of the pile bottom at the corresponding measuring points on both sides of the pile group shows a reverse relationship under the El-Centro horizontal earthquake excitations. If the negative value of earth pressure represents the compressive stress and the positive value represents the tensile stress, it means that one side of pile group foundation is under tension and the other side is under compression at the same time. The rotation effect of pile group foundation and pile cap will be caused by the antisymmetric tension compression of pile–soil contact pressure along the vertical direction, which results from the dynamic interaction of pile group-soil-structure system. For the pile group foundation system on the liquefiable foundation under the earthquake excitation, the lateral bearing capacity of the pile group

Rock and Soil Mechanics, Vol. 41 [2020], Iss. 3, Art. 6

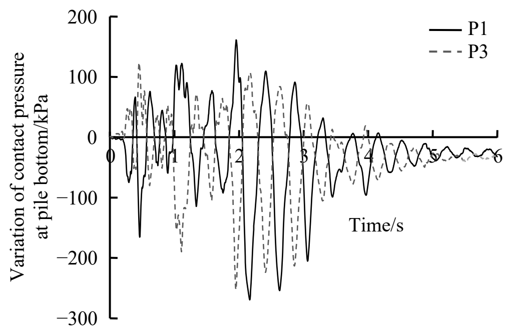

(a) P1、P3 under unidirectional earthquake excitations

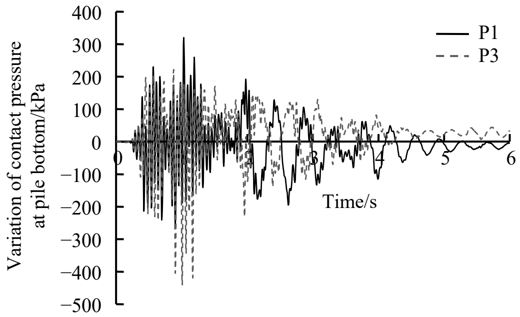

(b) P1、P3 under bidirectional coupling earthquake excitations

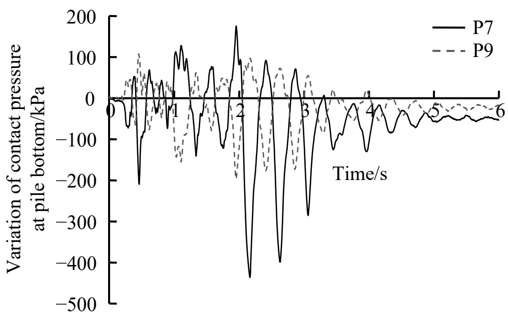

(c) P7、P9 under unidirectional earthquake excitations

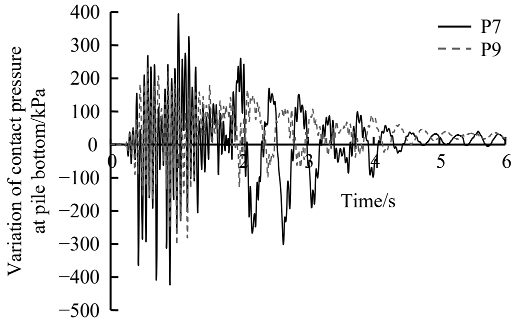

(d) P7、P9 under bidirectional coupling earthquake excitations

Fig.11 Plots of pile bottom contact pressure under El-Centro earthquake excitation at 0.76*g*

foundation will be greatly reduced after soil liquefaction, and at the same time, the compression and pull-out effect on both sides of the pile group foundation act together on the upper structure, which is the fundamental reason for the swaying, tilting and collapse of the pile group system of the building structure in the liquefiable region.

According to the analysis of Figs.11(b) and 11(d), the variation trends of the time history plots of the pile bottom earth pressure at the corresponding measuring points on both sides of the pile group foundation are the same, but the peak value of the earth pressure change and the frequency of the reciprocating transformation increase under the El-Centro bidirectional coupling earthquake excitations in the strong earthquake stage (0–2.1s). The peak values of the pile bottom earth pressure changes of piles P1 and P3 are 256 kPa and 440 kPa, respectively, and the increase rate is about 55.2%–73.9%, compared with the horizontal earthquake excitations. The peak values of the pile bottom earth pressure changes of piles P7 and P9 are 423 kPa and 303 kPa, respectively, and the increase rate is about 53.8%–101.4% compared with the horizontal earthquake excitations. This phenomenon is due to the increase of tension and compression of pile group foundation caused by horizontal and vertical coupling earthquake excitations.

4.3 Rotation effect of foundation

In general, most studies focus on the failure of components subjected to vertical forces under the bidirectional coupling earthquake excitations. Chen et al.[18] pointed out that due to the influence of soil–foundation–structure dynamic interaction, the structure will produce swaying component under earthquake excitations and cause the rotation effect of foundation. The relationship between the pull-out effect of pile group and the rotation of foundation has been preliminarily clarified by the analysis of pile bottom earth pressure in the previous analysis. In order to further study the influence of bidirectional coupling earthquake excitations on the rotation effect of pile group foundation in the interaction system, a pair of vertical accelerometers AZ1-1 and AZ1-2 are symmetrically placed at the top surface of pile group foundation in this test to specifically measure the rotation effect of foundation. According to the literatures[18–19], the angular rotational acceleration of pile group foundation is calculated as follows:

$$\ddot{\theta}_1 = \frac{\ddot{Z}_1 + \ddot{Z}_2}{L_1} \tag{1}$$

where L_1 is the distance between measuring points AZ1-1 and AZ1-2; $\ddot{Z}_1$, $\ddot{Z}_2$ are the measured vertical acceleration of measuring points AZ1-1 and AZ1-2, respectively.

Figure12 shows the rotational angular acceleration and Fourier spectrum of pile group foundation under the El-Centro earthquake excitation at 0.76*g*. A further comparison study found that the rotational angular acceleration and Fourier spectrum of the pile group foundation under different earthquake excitations are different, which are manifested in the following two aspects:

https://rocksoilmech.researchcommons.org/journal/vol41/iss3/6
DOI: 10.16285/j.rsm.2019.5306

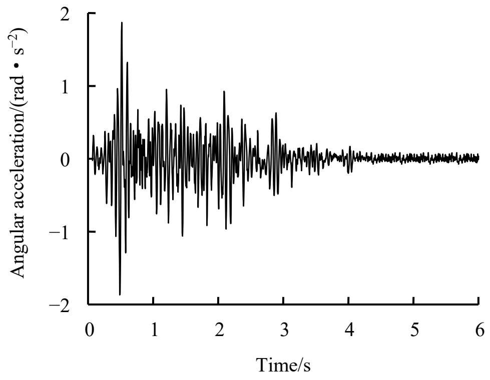

(a) Time history of angular acceleration under horizontal earthquake excitations

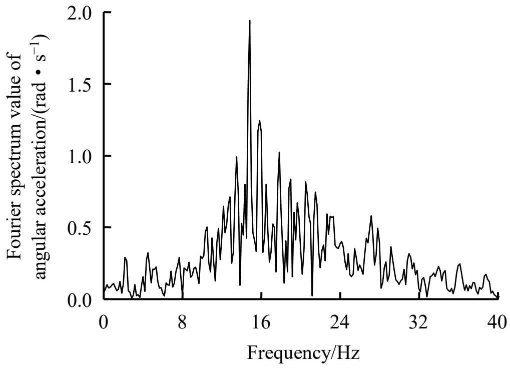

(b) Angular acceleration of Fourier spectrum–frequency curve under horizontal earthquake excitations

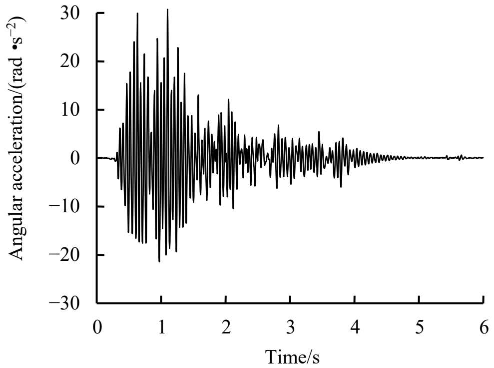

(c) Time history of angular acceleration and bidirectional coupling earthquake excitations

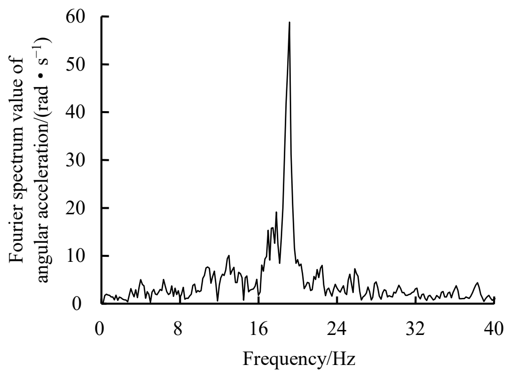

(d) Angular acceleration of Fourier spectrum–frequency curve under bidirectional coupling earthquake excitations

Fig.12 Time histories and Fourier spectra of rotational acceleration of foundation under El-Centro earthquake excitation at 0.76*g*

(1) The bidirectional coupling earthquake excitations have a significant amplification effect on the peak value of rotational angular acceleration of the pile group foundation. The peak value of the angular acceleration for foundation is 1.87 rad/s^2 under the El-Centro horizontal earthquake excitation at 0.76*g*, and 30.73 rad/s^2 under the El-Centro bidirectional coupling earthquake excitations at 0.76*g*, the latter is 16.43 times of the former, and the foundation rotation effect is more significant under the bidirectional coupling earthquake excitations.

(2) Compared with the horizontal earthquake excitations, the Fourier spectrum value of the rotation angular acceleration for foundation under the bidirectional coupling earthquake excitations has changed significantly. The main frequency of the response of the base rotational angular acceleration is 14.5–15.5 Hz under the El-Centro horizontal earthquake excitation at 0.76*g*, the main frequency range covers 10–28 Hz, corresponding to the 18.2–19.8 Hz of the response of the base rotational angular acceleration under the El-Centro bidirectional coupling earthquake excitations at 0.76*g*, and the main frequency range covers 16–23.8 Hz.

The above analysis shows that the rotation effect of the pile group foundation is obviously increased due to bidirectional coupling earthquake excitations. Compared with the horizontal earthquake excitations, the bidirectional coupling earthquake excitations exacerbated the swaying and tilting of the liquefiable pile group foundation during the earthquake excitations. Therefore, the adverse effects of bidirectional coupling earthquake excitations should be considered in engineering design.

5 Conclusions

Based on the shaking table model test of the dynamic interaction system of liquefiable ground–pile group–frame tube structure, the dynamic response of the liquefiable ground and pile group foundation under bidirectional coupling earthquake excitations was studied, and compared with the dynamic response of liquefiable ground and pile group under horizontal earthquake excitations, the following conclusions are obtained:

(1) For the vertical acceleration response of soil, the test soil can amplify the transmission of vertical vibration under bidirectional coupling earthquake excitations. During the propagation of vertical vibration from the bottom to the top of the soil, the peak value of acceleration keeps increasing, but its spectrum characteristics show no significant change.

(2) For the change of excess pore water pressure of saturated sand, the degree of liquefaction of saturated sand is related to the type of input earthquake motions and the bidirectional coupling earthquake excitations. Under the input of El-Centro earthquake motions, the bidirectional coupling

earthquake excitations can promote the liquefaction of sand; under the input of Kobe earthquake motions, the bidirectional coupling earthquake excitations have little effect on the liquefaction degree of sand.

(3) For the dynamic response of the pile foundation, the bidirectional coupling earthquake excitations not only increases the damage of the middle and bottom of the pile, but also have an important impact on the tension and compression of pile foundation and the rotation effect of the pile group foundation. The bidirectional coupling earthquake excitations exacerbate the swaying and tilting of the pile group system of the building structure.

(4) In the seismic design of pile foundations, it is necessary to consider the bidirectional coupling earthquake excitations, especially for the design of pile foundations on liquefiable ground, it is recommended to consider the adverse effects of the horizontal and vertical coupling earthquake excitations.

References

[1] CHEN Nian-ying. Significance of vertical earthquake effect by the thought of Hanshin earthquake of Japan[J]. Journal of Chengdu University(Natural Science Edition), 1996, 15(1): 56–59.

[2] ZHOU Zheng-hua, ZHOU Yong-nian, ZHAO Gang. Statistical analysis of peak ratios andresponse spectra of near-field accelerograms[J]. Earthquake Engineering and Engineering Vibration, 2002, 22(3): 15–18.

[3] FARSANGI E N, YANG T Y, TASNIMI A A. Influence of concurrent horizontal and vertical ground excitations on the collapse margins of non-ductile RC frame buildings. strength[J]. Structural Engineering and Mechanics, 2016, 59(4): 653–669.

[4] CHEN Y Z, KUN C, LARKIN T, et al. Impact of vertical ground excitation on a bridge with footing uplift[J]. Journal of Earthquake Engineering, 2016, 20(7): 1035–1053.

[5] TAN Zhen. Seismic performance analysis of tall chimney structure subjected to vertical and horizontal excitations[D]. Shanghai: Tongji University, 2007.

[6] ZHANG Yan-nian, LI Hong-nan. Seismic responses of sliding base-isolated structure under bidirectional coupling earthquake and its optimization[J]. Journal of Earthquake Engineering and Engineering Vibration, 2006, 27(1): 1–6.

[7] PRASAD S K, TOWHATA L. Shaking table tests in earthquake geotechnical engineering[J]. Current Science, 2004, 87(10): 1398–1404.

[8] WANG Z H, Duenas-OSORIO L, PADGETT J E. Seismic response of a bridges oil foundation system under the combined effect of vertical and horizontal ground motions[J]. Earthquake Engineering & Structural Dynamics, 2013, 42(4): 545–564.

[9] TSAPARLI V, Kontoe S, TABORDA DMG, et al. Vertical ground motion and its effects on liquefaction resistance of fully saturated sand deposits[J]. Proceedings of The Society A-Mathematical Physical and Engineering Sciences, 2016, 472(2192): 20160434.

[10] GUO Sheng-bing, ZHAO Yi, ZHAO Yue-tang, et al. Dynamic analysis of underground structures under the vertical and horizontal seismic load[J]. Underground Space, 2002, 22(4): 314–319.

[11] CHEN Yue-qing, LU Xi-lin, HUANG Wei. Simulation method of soil boundary condition in shaking table tests of soil–structure interaction[J]. Structural Engineers, 2000(3): 25–30.

[12] The Professional Standards Compilation Group of People's Republic of China. JGJ94－2008 Technical code for building pile foundations[S]. Beijing: China Architecture and Building Press, 2008.

[13] JIANG Yu-min, QIAN De-ling, ZHANG Ze-han, et al. Shaking table tests on dynamic interaction of frame-core tube structure and subgrade[J]. Journal of Building Structures, 2016, 37(2): 34–40.

[14] DAI Qi-quan, QIAN De-ling, ZHANG Ze-han, et al. Experimental research on dynamic response of pile group of super high rise building on liquefiable ground[J]. Chinese Journal of Rock Mechanics and Engineering, 2015, 34(12): 2572–2579.

[15] LING Xian-zhang, WANG Dong-sheng, WANG Zhi-qiang, et al. Large-scale shaking table model test of dynamic soil-pile-bridge structure interaction in ground of liquefaction[J]. China Civil Engineering Journal, 2004, 37(11): 67–72.

[16] LÜ Xi-lin, REN Hong-mei, LI Pei-zhen. Numerical analysis of free field system in liquefiable site and validation of shaking table tests[J]. Chinese Journal of Rock Mechanics and Engineering, 2009, 28(Suppl.2): 4046–4052.

[17] TANG Liang, LING Xian-zhang, XU Peng-ju, et al. Shaking table test on seismic response of pile groups of bridges in liquefiable ground[J]. Chinese Journal of Geotechnical Engineering, 2010, 32(5): 672–680.

[18] CHEN Yue-qing, LÜ Xi-lin, LI Pei-zhen. Effects of soil–structure interaction with various soils[J]. Journal of Wuhan University: Engineering and Technology Edition, 2005, 38(3): 63–68.

[19] YU Xu, ZHUANG Hai-yang, ZHU Chao. Shaking table model test for multi-story isolated structure on softer interlayer foundation[J]. Journal of Vibration and Shock, 2015, 34(24): 109–115.